

Inelastic Collisions of Ultracold Heteronuclear Molecules in an Optical Trap

Eric R. Hudson,^{1,*} Nathan B. Gilfoy,¹ S. Kotochigova,² Jeremy M. Sage,^{1,†} and D. DeMille¹

¹*Department of Physics, Yale University, 217 Prospect Street, New Haven, Connecticut 06511, USA*

²*Department of Physics, Temple University, Philadelphia, Pennsylvania 19122-6082, USA*

(Received 15 February 2008; published 20 May 2008)

Ultracold RbCs molecules in high-lying vibrational levels of the $a^3\Sigma^+$ ground electronic state are confined in an optical trap. Inelastic collision rates of these molecules with both Rb and Cs atoms are determined for individual vibrational levels, across an order of magnitude of binding energies. The long-range dispersion coefficients for the collision process are calculated and used in a model that accurately reproduce the observed scattering rates.

DOI: [10.1103/PhysRevLett.100.203201](https://doi.org/10.1103/PhysRevLett.100.203201)

PACS numbers: 37.10.Pq, 03.65.Nk, 33.80.-b, 34.50.-s

The electric dipole-dipole interaction provides a strong, long-range, tunable anisotropic interaction between polar molecules. This is fundamentally different from most interactions studied between ultracold atoms, which are typically isotropic and comparatively short-ranged. Features of the dipole-dipole interaction can lead to many novel and exciting phenomena, such as field-linked states [1], long-range topological order [2], quantum chemistry [3,4], and the possibility for quantum computation [5,6]. Furthermore, the presence of closely spaced internal levels of the molecules, e.g., Ω -doublet, rotational, and vibrational levels, presents a host of new possibilities for precision measurement of fundamental physics [7–10]. A trapped *ultracold* sample of polar molecules, which will provide high densities and long observation times, is thus a necessary step for observing these phenomena.

Techniques such as Stark deceleration [11] and buffer gas cooling [12] are capable of producing cold samples from a wide range of polar molecular species. However, the temperatures and densities currently attainable via these methods are limited. Conversely, the association of ultracold atoms, either via a Feshbach [13] or optical resonance [14], restricts experiments to molecules composed of laser-cooled atoms. Nonetheless, these methods are approaching temperatures and densities appropriate for observing the aforementioned phenomena.

In this Letter, we report the optical confinement of ultracold, vibrationally excited RbCs molecules in their $a^3\Sigma^+$ ground electronic state, produced via photo-association (PA) of laser-cooled ^{85}Rb and ^{133}Cs atoms. We utilize the long observation times afforded by the optical trap to determine the inelastic scattering rate for specific vibrational levels of these molecules, with both ^{85}Rb and ^{133}Cs atoms, across an order of magnitude of binding energies. We show that a conceptually simple model for the collision process accurately reproduces the observed scattering rates. We also extend this model to estimate molecule-molecule inelastic scattering rates, and discuss implications for producing trapped samples of $X^1\Sigma^+(v=0, J=0)$ RbCs molecules.

The apparatus used in this work is similar to that described in Ref. [15]. Briefly, ^{85}Rb and ^{133}Cs atoms are cooled and collected in a dual-species, forced dark-spot magneto-optical trap (DSM) [16]. Using absorption imaging along two orthogonal directions, we co-locate the species and measure the atomic density, n , and atom number, N , as $n_{\text{Rb}} = 4(2) \times 10^{11} \text{ cm}^{-3}$, $N_{\text{Rb}} = 9(1) \times 10^7$, and $n_{\text{Cs}} = 5(1) \times 10^{11} \text{ cm}^{-3}$, $N_{\text{Cs}} = 2(1) \times 10^8$. The temperature, T , of each species in the DSM was measured by time-of-flight expansion to be $T_{\text{Rb}} = 80(25) \mu\text{K}$ and $T_{\text{Cs}} = 105(40) \mu\text{K}$. Our optical trap is a quasidelectrostatic trap (QUEST), realized in a vertical 1-D lattice configuration by focusing and retro-reflecting a 70 W CO_2 laser beam (10.6 μm wavelength). An acousto-optic modulator placed in the beam path allows for the rapid turn-off of the QUEST ($\tau < 1 \mu\text{s}$). Because we utilize a lattice configuration for our QUEST, we are not restricted to trapping at the focus. We find it advantageous to move the point of overlap between the QUEST and DSM, so that we trap ~ 9 mm away from the focus. Here, the e^{-2} intensity beam waist is $\sim 400 \mu\text{m}$ (peak intensity of $\sim 110 \text{ kW/cm}^2$), and the trap depths are $\sim 150 \mu\text{K}$, $\sim 200 \mu\text{K}$, and $\sim 300 \mu\text{K}$ for Rb, Cs, and $a^3\Sigma^+$ RbCs, respectively. In addition to providing a larger trapping volume, this method mitigates the effects of QUEST-induced light shifts of the atomic states [17].

The energy level scheme relevant to the RbCs formation is shown in Fig. 1. The PA laser has an intensity of $\sim 2 \text{ kW/cm}^2$, and its frequency is locked to an $\Omega = 0^-$, $J^P = 1^+$ level, located 38.02 cm^{-1} below the Rb $5S_{1/2}(F=2) + \text{Cs } 6P_{1/2}(F=3)$ atomic asymptote [14]. Spontaneous decay of this state produces molecules in the $a^3\Sigma^+$ state, primarily in the vibrational level with binding energy $E_B = -5.0 \pm 0.6 \text{ cm}^{-1}$, to which we assign vibrational number v_0 . In our previous Letter [18], we tentatively assigned $v_0 = 37$, but this value has an uncertainty of several units since the depth of the $a^3\Sigma^+$ state potential well is not accurately known.

Data are taken by loading the DSM for 5 s from background alkali vapor, provided by heated getters, in the

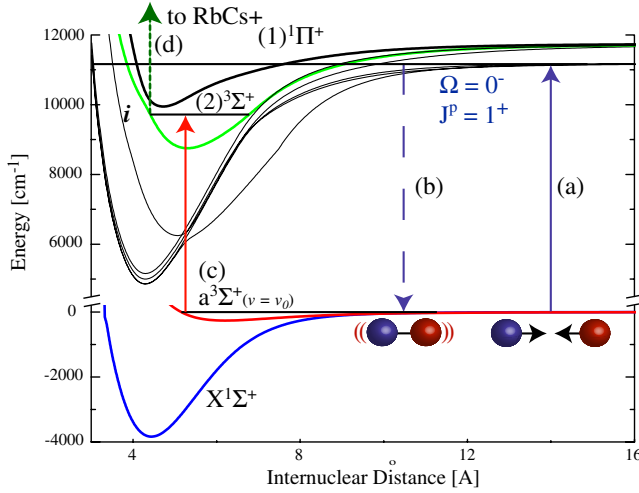


FIG. 1 (color online). Formation and detection processes for ultracold RbCs. (a) The PA laser excites colliding atom pairs into bound RbCs* molecules, which (b) decay into a range of vibrational states of the $a^3\Sigma$ potential. (c) $a^3\Sigma(v)$ molecules are excited to level i , then (d) ionized and detected.

presence of both the PA laser and QUEST. Atoms are not efficiently loaded into the lattice directly from the DSM, due to the low trap depth away from the focus. Because the QUEST is substantially deeper for the molecules than the atoms, the PA process efficiently loads RbCs into the lattice as the molecules are formed. From the measured atomic densities and known PA rates [18], we estimate that we trap $N_{\text{RbCs}} \approx 10^5$ molecules at density $n_{\text{RbCs}} \approx 10^9 \text{ cm}^{-3}$ and temperature $T_{\text{RbCs}} \approx 250 \mu\text{K}$, with roughly 30% in the $a^3\Sigma^+(v=v_0)$ state. The slight heating of molecules relative to atoms occurs during the loading process since the molecules are more strongly trapped.

To study atom-molecule collisions, we load atoms into the lattice more efficiently via an optical molasses cooling stage for the desired atomic species, after the DSM is loaded. The optical molasses stage is performed by shifting the detunings, Δ , of the DSM trap lasers to $\Delta_{\text{Rb}} = -6\Gamma$, $\Delta_{\text{Cs}} = -16\Gamma$ for 10 ms, where Γ is the transition natural linewidth. The DSM hyperfine repumping beam is extinguished for the last 100 μs of the molasses stage to ensure that all trapped atoms are in the lowest (dark) hyperfine state. Loading the lattice in this way leads to typical densities $n_{\text{Rb}} = 2(1) \times 10^{11} \text{ cm}^{-3}$ and $n_{\text{Cs}} = 6(1) \times 10^{11} \text{ cm}^{-3}$, and temperatures $T_{\text{Rb}} = 20(11) \mu\text{K}$ and $T_{\text{Cs}} = 20(15) \mu\text{K}$ in a volume $V \approx 3 \times 10^{-5} \text{ cm}^3$. This is roughly a factor of 40 increase in density and factor of 5 reduction in temperature compared to loading the lattice directly from the DSM. After the molasses stage, we apply resonant “push”-beams for 10 ms to remove any undesired atoms from the lattice. After the “push”-beam sequence, all non-lattice beams are shuttered, leaving the molecules and any desired atoms trapped.

After a variable delay time, the QUEST is switched off, and the trapped molecules are state-selectively ionized

using Resonance-Enhanced Multi-Photon Ionization (REMPI). The resulting ions are detected using time-of-flight mass spectrometry [15]. In this manner, we use the observed trap-lifetime of the molecules in the QUEST as a direct measurement of the molecular collision rates.

Typical lifetime data is shown in Fig. 2 for molecules in the $a^3\Sigma^+(v=v_0)$ state. As can be seen, the presence of atoms in the lattice significantly shortens the lifetime of the trapped molecules, which is otherwise limited by collisions with background gas. We attribute this behavior to inelastic collisions between the atoms and molecules. These losses are likely due to rovibrational quenching or hyperfine-changing collisions. Relaxation of each of these degrees of freedom liberates enough kinetic energy to remove both the molecule and the atom from the trap.

The number of trapped molecules, N_{RbCs} , evolves as

$$\frac{dN_{\text{RbCs}}}{dt} = -(\Gamma_{\text{BG}} + \Gamma_{\text{atom}})N_{\text{RbCs}} - \frac{\beta}{V}N_{\text{RbCs}}^2.$$

Here, Γ_{BG} is the loss rate due to collisions with background gas, Γ_{atom} is the loss rate due to inelastic collisions with atoms, β is the molecular 2-body loss rate, and V is the trap volume occupied by the molecules. Under our present conditions, two-body processes are negligible compared with background gas collisions ($\beta n_{\text{RbCs}}/\Gamma_{\text{BG}} \ll 1$). Hence, we fit the data to the form $N_{\text{RbCs}}(t) = N_0 e^{-t/\tau}$ with $\tau^{-1} = \Gamma_{\text{atom}} + \Gamma_{\text{BG}}$, to extract the value of Γ_{atom} . Γ_{atom} is related to the energy-dependent inelastic cross section, $\sigma(E)$, and the relative velocity, v , as $\Gamma_{\text{atom}} = n_{\text{atom}} \langle \sigma(E)v \rangle$, where $\langle \rangle$ denotes thermal averaging.

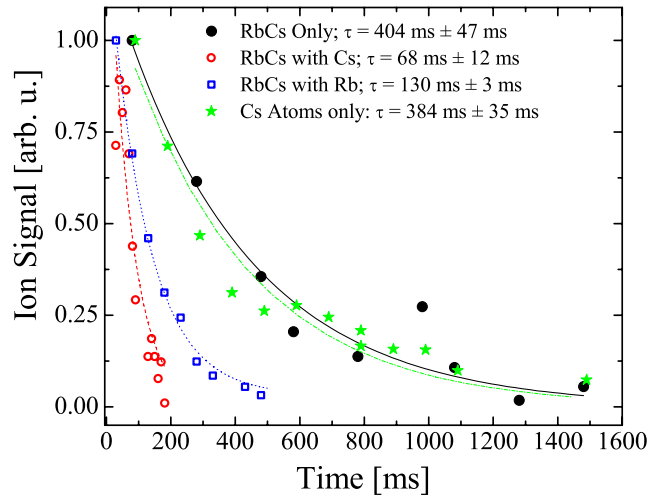


FIG. 2 (color online). Typical molecular lifetime data. Here, the number of molecules in the $a^3\Sigma^+(v=v_0)$ state with binding energy $E_B = -5.0 \pm 0.6 \text{ cm}^{-1}$ is observed in the QUEST as a function of time. The presence of inelastic collisions between the atoms and molecules is evidenced by the dramatic reduction of the molecular lifetime when atoms are present. With no atoms present, we observe molecule lifetimes consistent with the background gas-limited lifetime seen for isolated atomic clouds in the trap.

Hence, knowledge of the densities and temperatures allows the determination of the scattering rate constant, $K(T) = \langle \sigma(E)v \rangle$.

The initial PA process populates several vibrational states in the $a^3\Sigma^+$ state. We utilize the state-selectivity provided by the REMPI detection to measure data similar to that in Fig. 2, for several different vibrational states with binding energies in the range $E_B \approx -0.5 \text{ cm}^{-1}$ to -7 cm^{-1} (measured relative to the $a^3\Sigma^+$ asymptote). The results of these measurements are summarized in Fig. 3. The error bars on each point are dominated by systematic uncertainty in determining the trap volume of the molecules, since they are loaded into the lattice at a different temperature than the atoms. The range of the molecular trap volume, reflected in the error bars, is bounded by the measured atomic trap volumes and the DSM volume. The measured rate constants are identical within experimental precision, despite over an order of magnitude of variation in E_B . Since the molecule size and rovibrational energy spacing both change substantially over this range of E_B , the lack of dependence of the scattering rate on molecular binding energy hints at a process where the details of the short-range interaction potential are unimportant. This view is supported by the agreement of the data with the results of a conceptually simple model of the collision process, shown in Fig. 3 as hatched boxes. This model [19], which is detailed below, assumes that any collision which penetrates to short-range results in an inelastic trap loss event.

For two colliding particles, the energy-dependent scattering cross section for the ℓ th partial wave, with projection m , from state i to state f in all outgoing partial waves ℓ', m' is generally written as

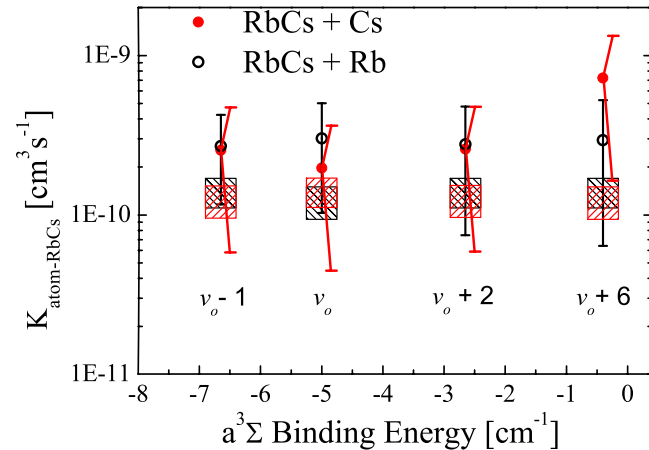


FIG. 3 (color online). Molecular trap-loss scattering rate constant K vs binding energy E_B , for molecules in specific vibrational levels of the $a^3\Sigma^+$ state. Vibrational state label appears below each data point. The black (red) crosshatched box is the prediction of the model described in the text for collisions with Cs (Rb). The width of the boxes reflects the uncertainty in the collision temperature.

$$\sigma_{\ell,m}(E, i \rightarrow f) = \frac{\pi}{k^2} \sum_{\ell',m'} |T_{\ell,m,\ell',m'}(E, i \rightarrow f)|^2.$$

Here, $T_{\ell,m,\ell',m'}(E, i \rightarrow f)$ represents the probability amplitude for a transition from the incoming spherical wave $\Psi_{i,\ell,m}$ to the outgoing wave $\Psi_{f,\ell',m'}$, and $k = \sqrt{2\mu E/\hbar^2}$ is the magnitude of the wave vector with collision energy E and reduced mass μ . Since our experiments are sensitive to the total cross section for collisions that remove molecules from the trap, we must sum over all final states f that lead to trap loss, in addition to the normal sum over l, m . If we assume that any collision that penetrates to short-range is inelastic with unit probability, we can write the total cross section as

$$\sigma(E, i) = \sum_{f,\ell,m} \sigma_{\ell,m}(E, i \rightarrow f) = \sum_{\ell} \frac{\pi}{k^2} (2\ell + 1) P_T(E, \ell),$$

where $P_T(E, \ell)$ is the probability of transmission to short-range. We calculate $P_T(E, \ell)$ by numerically solving the Schrödinger equation for the long-range potential, and assuming any flux not reflected off the potential is transmitted to short-range and then completely lost to inelastic processes. This technique is applicable to any highly-inelastic process; it requires only the knowledge of the long-range part of the scattering potential.

In our case, the long-range potential, $V(r, \ell) = \frac{\hbar^2 \ell(\ell+1)}{2\mu r^2} - \frac{C_6}{r^6}$, is determined entirely by the value of μ and the van der Waals coefficient, C_6 ; this is valid for particle separation $r \geq 10 \text{ \AA}$. In general, the C_6 constant for two colliding particles is given by the integral over imaginary frequency of the product of the particles' dynamic polarizabilities [20]. Based on the approach developed in Ref. [21], we have calculated the dynamic polarizability of the atoms and molecules. Using these values, we determine the v -dependent C_6 constants, shown in Table I.

P_T , σ , and K are calculated from the determined C_6 values for Rb + RbCs, Cs + RbCs, and RbCs + RbCs collisions. The results are shown in Fig. 4. The collision rates fall to the values given solely by their s -wave contribution at the lowest energies on the graph. As expected, quantum reflection from the $\ell = 0$ potential is found to scale linearly with k as $E \rightarrow 0$, consistent with the Wigner threshold law for low temperature inelastic scattering of $\sigma \propto 1/k$ [22], i.e., $\Gamma \rightarrow \text{const}$ as $E \rightarrow 0$. From the predicted molecule-molecule scattering rate, we expect an

TABLE I. Calculated C_6 coefficients for $a^3\Sigma^+$ RbCs(v) collisions with various partners given in atomic units.

Collision Type	$(v_0 - 1)$	(v_0)	$(v_0 + 2)$	$(v_0 + 6)$
RbCs(v) + RbCs(v)	65745	65086	64310	61291
Rb + RbCs	16991	16920	16869	15960
Cs + RbCs	19688	19604	19541	18482

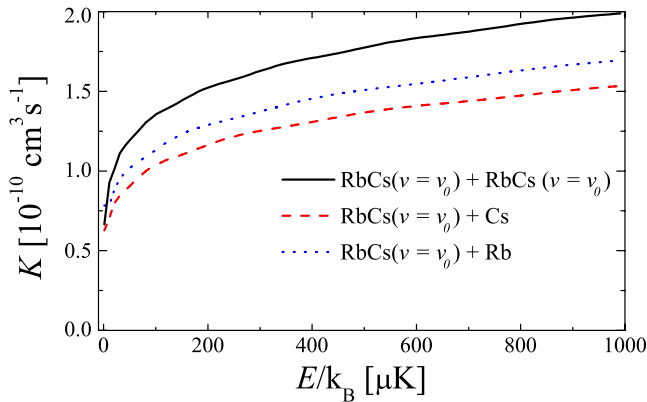


FIG. 4 (color online). Numerically calculated scattering rate constant K vs center-of-mass frame collision energy E for atom-molecule and molecule-molecule collisions.

initial two-body loss rate of $\frac{\beta}{V} N_{\text{RbCs}} = 2Kn_{\text{RbCs}} \approx 0.2$ Hz. Since $\Gamma_{\text{BG}} \approx 2$ Hz under present conditions, our measurement of background gas-limited decay for the pure RbCs sample is consistent with the predicted scattering rate. With planned improvements, we expect to directly observe molecule-molecule collisions in the near future.

In conclusion, we have demonstrated the trapping of ultracold RbCs molecules in vibrationally excited levels of the $a^3\Sigma^+$ electronic ground state. Observations of the molecules in the trap have revealed strong inelastic collisions. In contrast to previous work with homonuclear molecules [23,24], this work is the first measurement of ultracold collisions with trapped, photo-associated heteronuclear molecules, and thus represents a crucial step towards trapped, ground state ultracold polar molecules. Furthermore, unlike work with Feshbach-associated molecules [13], we have utilized state-sensitive detection to determine the molecular inelastic scattering rate with two species of atoms for specific vibrational states with a wide range of binding energy. Additionally, we have developed a model that relies only on knowledge of the van der Waals coefficient, which accurately reproduces the observed rates. By assuming that only short-range collisions are inelastic, this model represents a more realistic description of the scattering process than the previously used s -wave unitarity limit [23].

We are currently working towards transferring these trapped molecules into their absolute ground state, via the scheme previously demonstrated in our lab [15]. It appears that with minimal improvements, e.g., implementing an adiabatic transfer [25] instead of the stimulated emission pumping used in [15], a sample of $>10^4$ absolute ground state molecules [$X^1\Sigma^+(v=0, J=0)$] at a temperature of $20 \mu\text{K}$ and density of $\geq 10^9 \text{ cm}^{-3}$ can be created. From calculations based on the available laser powers, we estimate the transfer process can take place in $\leq 100 \mu\text{s}$; thus, we anticipate negligible loss of popula-

tion due to the inelastic collisions studied in the present work. In fact, these inelastic collisions could serve a useful purpose. If Cs atoms are deliberately loaded into the lattice, any molecule not in the absolute ground state will quickly (~ 100 ms) be removed from the trap by these inelastic collisions. By contrast, $X^1\Sigma^+(v=0, J=0)$ molecules, which cannot undergo inelastic collisions with Cs atoms, are unaffected by the presence of the atoms. [Note that even ground state molecules can have inelastic collisions with Rb atoms via the energetically allowed substitution reaction $\text{RbCs} + \text{Rb} \rightarrow \text{Rb}_2 + \text{Cs}$]. After the excited state molecules have been removed, resonant “push”-beams can eject the remaining atoms from the trap, leaving behind a pure sample of $X^1\Sigma^+(v=0, J=0)$ molecules.

We thank H. Sadeghpour for stimulating discussions regarding the calculation of C_6 coefficients. This work was supported by DOE, ARO, and NSF Grants Nos. DMR0325580, W911NF0510472, and PHY0354211.

*Eric.Hudson@Yale.edu

†Present Address: Lincoln Laboratory, Massachusetts Institute of Technology, Lexington, MA, 02420, USA

- [1] A. V. Avdeenkov, D. C. E. Bortolotti, and J. L. Bohn, *Phys. Rev. A* **69**, 012710 (2004).
- [2] A. Micheli, G. K. Brennen, and P. Zoller, *Nature Phys.* **2**, 341 (2006).
- [3] R. V. Krems, *Int. Rev. Phys. Chem.* **24**, 99 (2005).
- [4] E. R. Hudson *et al.*, *Phys. Rev. A* **73**, 063404 (2006).
- [5] D. DeMille, *Phys. Rev. Lett.* **88**, 067901 (2002).
- [6] P. Rabi *et al.*, *Phys. Rev. Lett.* **97**, 033003 (2006).
- [7] E. R. Hudson *et al.*, *Phys. Rev. Lett.* **96**, 143004 (2006).
- [8] D. DeMille *et al.*, *Phys. Rev. Lett.* **100**, 023003 (2008).
- [9] D. DeMille *et al.*, *Phys. Rev. Lett.* **100**, 043202 (2008).
- [10] T. Zelevinsky, S. Kotochigova, and J. Ye, *Phys. Rev. Lett.* **100**, 043201 (2008).
- [11] H. L. Bethlem, G. Berden, and G. Meijer, *Phys. Rev. Lett.* **83**, 1558 (1999).
- [12] J. M. Doyle *et al.*, *Phys. Rev. A* **52**, R2515 (1995).
- [13] C. Ospelkaus *et al.*, *Phys. Rev. Lett.* **97**, 120402 (2006).
- [14] A. Kerman *et al.*, *Phys. Rev. Lett.* **92**, 033004 (2004).
- [15] J. M. Sage *et al.*, *Phys. Rev. Lett.* **94**, 203001 (2005).
- [16] M. H. Anderson *et al.*, *Phys. Rev. A* **50**, R3597 (1994).
- [17] P. F. Griffin *et al.*, *New J. Phys.* **8**, 11 (2006).
- [18] A. Kerman *et al.*, *Phys. Rev. Lett.* **92**, 153001 (2004).
- [19] C. Orzel *et al.*, *Phys. Rev. A* **59**, 1926 (1999).
- [20] M. Marinescu, H. R. Sadeghpour, and A. Dalgarno, *Phys. Rev. A* **49**, 982 (1994).
- [21] S. Kotochigova and E. Tiesinga, *Phys. Rev. A* **73**, 041405 (2006).
- [22] N. Balakrishnan, R. Forrey, and A. Dalgarno, *Chem. Phys. Lett.* **280**, 1 (1997).
- [23] P. Staunum *et al.*, *Phys. Rev. Lett.* **96**, 023201 (2006).
- [24] N. Zahzam *et al.*, *Phys. Rev. Lett.* **96**, 023202 (2006).
- [25] K. Bergmann, H. Theuer, and B. W. Shore, *Rev. Mod. Phys.* **70**, 1003 (1998).